Advances in constitutive modelling of jointed rock hydro mechanical interactions at laboratory scale

Philippe LOPEZ[(1)], Alain THORAVAL[(2)], Olivier BUZZI[(3)], Iraj RAHMANI[(4)] & Marc BOULON[(5)]

(1) INPL-LAEGO-ENSMN, Parc de Saurupt, Ecole des mines, 54000 Nancy, France)
(2) INERIS, Parc de Saurupt, Ecole des mines, 54000 Nancy, France
(3) University of Newcastle, Australia
(4) Transportation Research Institute, No. 19, Noor Street,
Afrigha avenue, Tehran, Iran
(5) Laboratoire 3S (Sols, Solides, Structures), UMR 5521 (UJF, INPG, CNRS), 38041 Grenoble, France
Philippe.lopez@mines.inpl-nancy.fr

Abtract:

This study is a part of a wide multi scale research based on in situ *experimentations and laboratory tests. The latest, radial water injections in the centre of the lower joint wall are done at constant normal stress from 0 to 110 MPa and at pressures from 0 to 4 MPa. Four hydro mechanical tests have been performed at the L3S laboratory on fractured limestone samples (two diaclase and two bedding plane). The measurement analysis shows a relation between the contact surface variations and the flow values inside the fracture. The hydro mechanical modelling performed using 3DEC code can be improved from the previous analysis through the modification of the relation between the joint hydraulic opening and the joint mechanical closure. The remaining gap between simulations and measurements can be related to fracture asperity degradation and turbulent flow that have not been taken into account in the modelling.*

Résumé :

Cette étude s'inscrit dans une recherche multi échelles basée sur des expérimentations in situ *et des essais de laboratoire. Les essais, injections radiales d'eau au centre de l'éponte inférieure, sont fait à contrainte normale constante de 0 à 110 MPa et pour des pressions de 0 à 4 MPa. Quatre essais hydromécaniques ont été réalisés au laboratoire L3S sur des échantillons de calcaire fracturé (deux diaclases et deux joints de stratification). L'analyse des mesures montre une corrélation entre les variations de la surface de contact et le débit hydraulique dans la fracture. La modélisation hydromécanique réalisée à l'aide du code 3DEC peut être améliorée à partir de l'analyse précédente à travers la modification de la relation entre l'ouverture hydraulique et la fermeture mécanique du joint. L'écart entre les valeurs mesurées et calculées est lié en particulier à la dégradation des aspérités de la fracture sous forte contrainte et à la turbulence des écoulements non prises en compte dans la modélisation.*

Key-words : hydromechanics, interaction, morphology.

1 Introduction

When normal stress is applied on joints, the normal deformation is typically non linear. Goodman (1974) and Barton *et al*. (1985) proposed two different hyperbolic models, widely used nowadays. Evans *et al*. (1992) proposed a logarithmic model to explain the non linear normal closure behaviour of rock joints. These three major works indicate that the fracture stiffness increases as normal stress increases. Lately, Lee and Harrison (2001) used empirical parameters for non-linear fracture stiffness modelling. Furthermore, the research to link morphology with the mechanical behaviour improves, for example, in Huang *et al.* (2002) work, where a mathematical model is developed for regular asperities, the deformation behaviour of a rock joint explicitly accounts for the effects of joint surface morphology. For hydraulic behaviour, a commonly used equation is the cubic law. It is derived from the fundamental principle of dynamic and is applied to a particular geometry such as a parallel plate fracture. It

gives an analytical expression where the flow rate is depending on the pressure gradient and the cubic fracture aperture. Qian *et al.* (2005) obtained results from tests that indicate a non-Darcian turbulent flow in the fracture even though the Reynolds number was relatively low. Since the sixties, the hydro mechanical behaviour under normal closure has been widely studied. Londe and Sabarly (1966), using experimental results, showed a decrease in fracture transmissivity with normal stress. Witherspoon *et al*. (1980) proposed a modified cubic law, introducing a factor that accounts for the roughness of the fracture surface. Barton *et al*. (1985) proposed an empirical model with their JRC. There has been conflicting laboratory evidence about the cubic law and the effects of contact areas. An extensive study has been presented in details in the Rutqvist and Stephansson (2003) review article. The friction factor has been introduced in a lot of different laws, with or without an exponent. A recent paper, Nazridoust *et al.* (2006), show another empirical law in the case of laminar flow through a rock fracture. The point is that it is not representing a clear roughness measurement. In rock fractures the Therzagi effective stress concept is improved with considering the pressure applied to the surface contact proportion. The major objective of this work is to introduce a reel measurement of the morphology in the classical laws linking the hydraulic opening with normal displacement, and the normal stress with the fluid pressure.

2 Laboratory tests

A series of laboratory tests and a monitoring of the evolution of the morphology have been performed on diaclase and bedding plane samples of limestone. The samples have been chosen from boreholes drilled into the limestone of the Coaraze site, close to Nice, France. The site is a medium sized superficial limestone bedrock reservoir (roughly 20m by 20m by 20m) with diaclases and bedding planes. For site experiment purpose, quite a lot of drillings have been performed; rock and joint samples (diaclases and bedding planes) can be used for laboratory experiments. F1 and F2 are diaclase samples; JS1 and JS2 are bedding plane samples. The rock matrix is characterized by a Poisson's coefficient (ν) of 0.3, a Young's modulus and a normal strength with dispersive values: in the same direction of foliation 45 MPa<E<62 MPa and 86 MPa<σ_c<173 MPa. The tests have been performed on the prototype developed at the Laboratory 3S and called BCR3D (3D Direct shear box for Rock Joints) allows to investigate the hydro mechanical behaviour of rock joints and the flow anisotropy (Boulon 1995, Hans et al. 2003). Figure 1 provides a general view of the device.

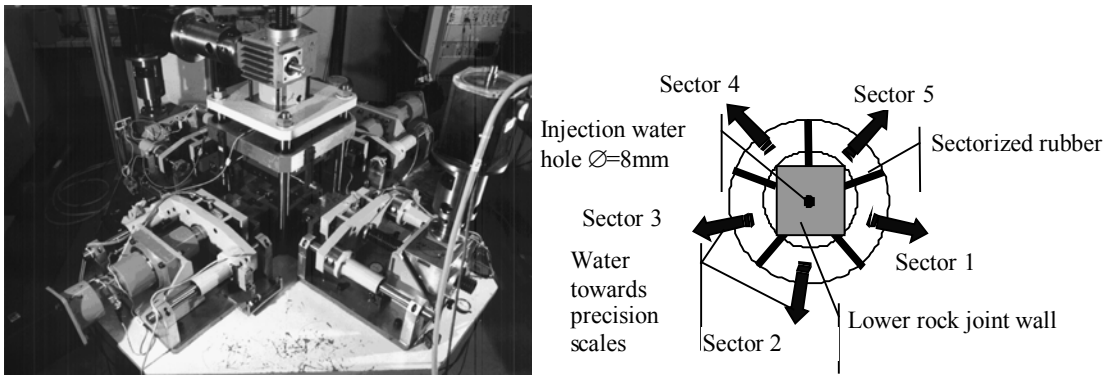

Figure 1. General front view and hydraulic part of the BCR3D.

The morphology (x,y,z) of both joint walls can be measured by a laser beam (diameter of the beam: 0.25 mm, sampling step: 0.15 mm/128 x 128 points over a maximum surface of 110 mm per 110 mm, vertical resolution: 0.01 mm). The laser can be placed in the BCR3D to scan the surfaces so that it is not necessary to remove the sample from the shear box (Figure 2). The

procedure allows both joint walls to stay aligned and prevents from the matching problems at the beginning of each part of tests. The physical values measured during a test are the normal relative displacement, the normal stress and the hydraulic parameters (the injection flow rate, the injection pressure and five outlet masses). The tests are performed according to the ISRM recommendations (Boulon, 1995). In this study, different steps of normal load are applied (loading velocity of 0.3 MPa/s) and some hydraulic excursions are performed at constant normal stress, *i.e.* increase and decrease of fluid pressure. While the stress level is constant, the water pressure rises following sills, from 0 to a maximum value; the relative normal displacement, the injection flow rate and the five output pressures are measured. For each value of the normal stress, an asymptotic value of the injection and output flow rate are reached.

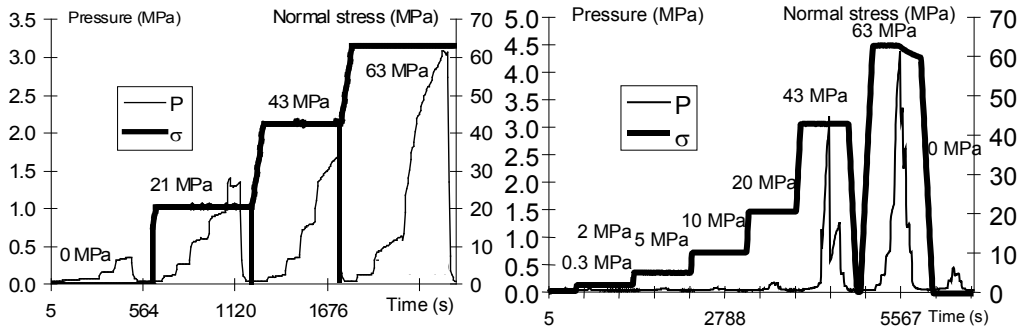

Figure 2: Applied stress and injection hydraulic pressure for F1 (left) and JS1 (right) samples.

For each morphology measurements two series of points (x,y,z) are known, one for the upper wall and one for the lower wall. After the upper wall has been flipped upside down and the joint walls aligned like they are along the test, it is possible to compute on each point the void space; it is compute, at a given loading stage of known normal stress and relative displacement (δ, σ_v), assuming that the deformation of an asperity does not influence the surrounding ones, and that the average displacement is also the displacement for each point of the joint walls. Figure 3 shows, for F1, the evolution of σ_n against u_n and the quite constant evolution of the normal stiffness (k_n) regarding the four different samples. The diaclases samples (F1 and F2) have higher normal stiffness than the bedding plane samples (JS1 and JS2) for normal stress higher than 20 MPa. At 60 MPa, the average value of diaclase normal stiffness is twice the value for the bedding planes (250 GPa/m and 125 GPa/m). So the bedding planes are easier to be closed than the diaclases. This can be inferred by the values of the classical roughness parameters, the range and the coefficient of variation of the height.

Table 1 shows the values for F1 and JS1. The stabilised flow rate value have been taken for each couple (σ_n; P_{inj}), Figure 4. For each value of the normal stress, the increase of the flow rate seems to be proportional to the injection pressure.

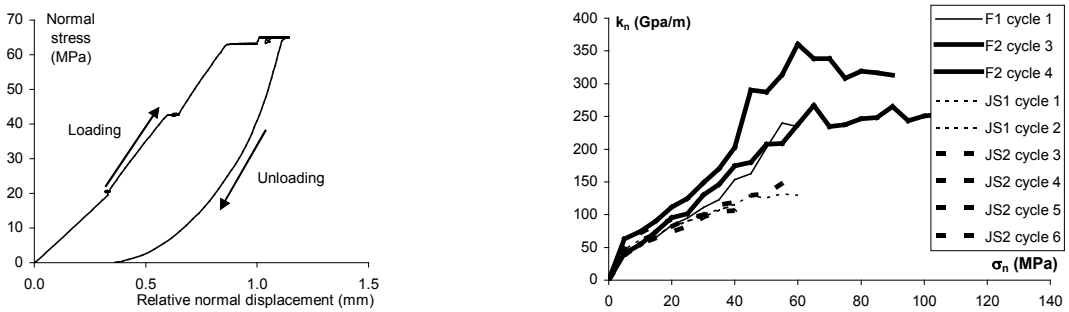

Figure 3. σ_n against u_n for F1 sample (left) and k_n against σ_n for all samples (right).

	CLA	RMS	Range	Coef Variation
F1	3.08	3.12	3.5	0.16
JS1	4.31	4.52	8.5	0.31

Table 1. Roughness coefficients of F1 and JS1.

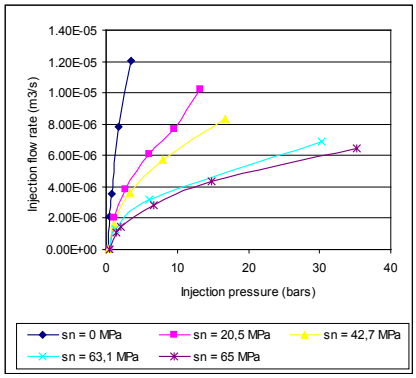

Figure 4. Injection flow rate/injection pressure.

3 Results and discussion

3.1 Hydro mechanical interpretations

A basic analytical interpretation of these tests, assuming laminar and isotropic flow between two parallel joint walls, allows estimating the initial openings of the discontinuities. The intrinsic transmissivity ($T_i=K_ie$), with a radial flow, take then the form of Equation 1.

$$Equation\ 1\ T_i = \frac{Q\mu_w}{P2\pi}\ln\left(\frac{r_e}{r_i}\right)\ with:\ 2\times r_e\ the\ external\ diameter,\ 2\times r_i\ the\ internal\ diameter.$$

The values of intrinsic transmissivity, measured for steady-state flow for each couple (σ_n ; P_{inj}), are in Figure 5.

Assuming moreover that the following relation between intrinsic transmissivity and hydraulic aperture: $Ti=a^3/12$, the hydraulic opening can be computed as in Equation 2. Figure 5 shows that the hydraulic openings decrease as the normal stress value increases. These values are all around 5.10^{-5} m, from 1.10^{-4} m down to 1.10^{-5} m (as the normal relative closure is related to the normal stress and the hydraulic opening). For high normal stress values, such as 90 and 110 MPa for sample F2, the hydraulic opening remains stable for injection pressures from 0 to 4 MPa. Whereas, for low normal stress, it decreases from 4.10^{-5} m down to 3.10^{-5} m. This phenomenon can be explained by the increase of Reynolds number, as much as the flow is no longer permanent but becomes turbulent.

At very low normal stress, up to 5 MPa, Figure 5 show that the hydraulic opening raise up for an increase of injection pressure. This phenomenon is observed for low injection pressure, at the beginning of the injection.

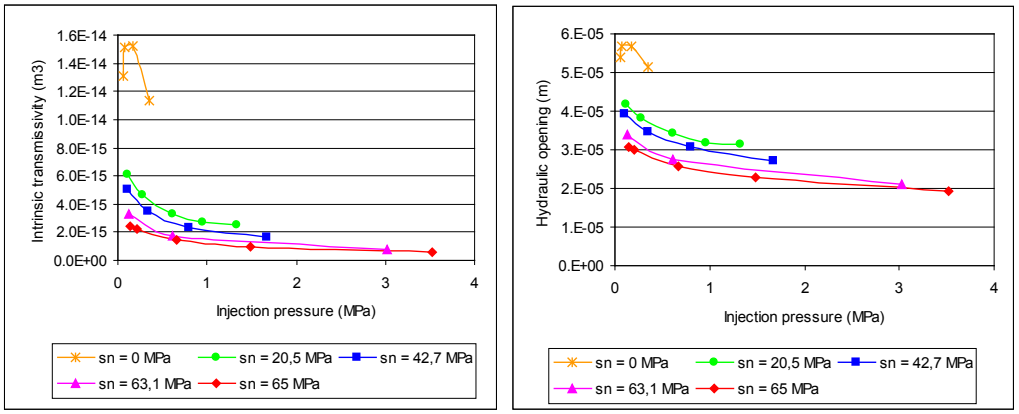

Figure 5. Intrinsic transmissivity and hydraulic opening against injection pressure for F1.

Equation 2

$$a = \sqrt[3]{\frac{Q6\mu_w}{P\pi}\ln\left(\frac{r_e}{r_i}\right)}$$

3.2 Morphology monitoring and hydro mechanical interactions

As we can back calculate the void space for each step of a test, we can study the interaction between morpho and hydro mechanical parameters. The surface is supposed to be in contact if the void space value is less than 0.001 mm. For each sector, the mean value δ_{mean}, standard deviation, and the coefficient of variation δ_{cv} (standard deviation divided by the average) of fracture openings is computed, and compared to the outflow rate, Figure 6. The comparison between the back calculated openings and the outflow rate are made when the flow is quasi permanent. The mean values of the openings do not follow the output flow (same figures, δ_{mean} compared to Q_{out}). Figure 6 shows that for F1 the proportion of the outflow for each sector does not depend on the normal stress level. We can assume three reasons to explain this difference:

- Tortuosity of the flow: it is not sectorised when the openings are sectorised; the flow is not only radial. The different channels that we could imagine on Figure 6 level 63 MPa, can drag a part of the flow towards sectors that do not have the maximum average opening, sector 1,
- From normal stress value 60 MPa, the hypothesis of independence between too contiguous asperities is no longer acceptable, there is damaging of the two joint walls,
- The behaviour, e.g. elasto-plastic, can no longer be ignored to back calculate the openings.

The coefficient of variation δ_{cv} is always increasing with the normal stress (Figure 7). The contact surface (S_c) values (Figure 8) are compared to the f coefficient define by $f = \Delta a/\Delta u_n$, where a is the hydraulic opening and u_n the normal mechanical opening. For JS1 and F1 the variation of f is the same. The f highest values are reached when the contact surface values increase. The main reason of the differences is the turbulent flow. The Reynolds number $Re = V D_h \rho/\mu$ with D_h hydraulic diameter (2a), ρ volumetric mass of water: 1000 kg/m^3, μ: dynamic viscosity: 10^{-3} Pa.s, V: flow speed (computed as a parallel flow Q_i / a*2*π*r_i where Q_i is the injection flow rate and r_i is the injection diameter tube), Equation 3.

Equation 3

$$\mathrm{Re} = Q_i \cdot \rho / \pi \cdot r_i \cdot \mu = \left(Q_i / r_i\right) \cdot 318471$$

For F1, the flow rate goes from 6.10^{-6} up to $1.2.10^{-5}$ m^3/s, ri = $2.5.10^{-3}$ m, the Reynolds number goes from 760 up to 1520. For JS1, as the maximum flow rate goes up to 2.10^{-5} m^3/s, the Reynolds number maximum value is 2547. Inside the sample, the flow rate can have higher values. Furthermore, the opening values are scattered. There are zones where Reynolds numbers are higher than the typical value of 2300. There is also a re-circulation phenomenon: it occurs when the opening increases suddenly (step phenomenon). So, there is turbulent flow in general, and locally this turbulent flow can be important.

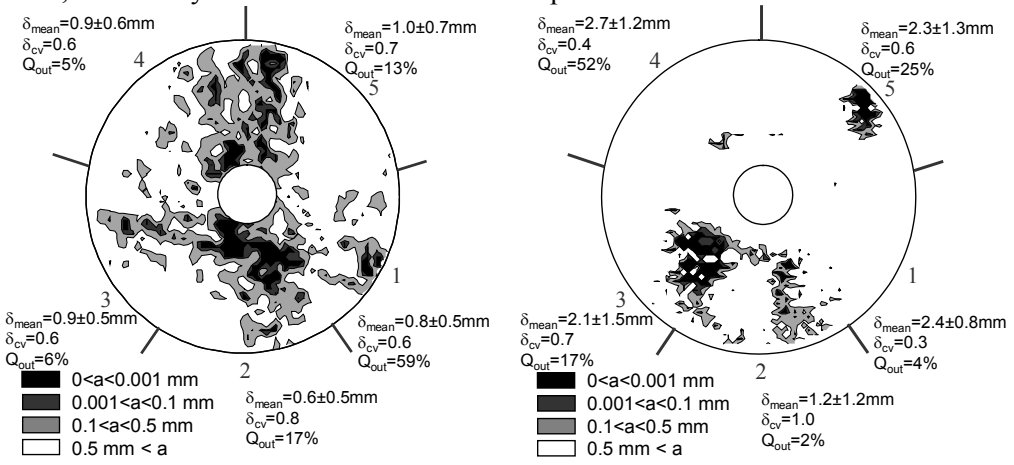

Figure 6. F1 Morpho-hydro-mechanical scheme 63 MPa

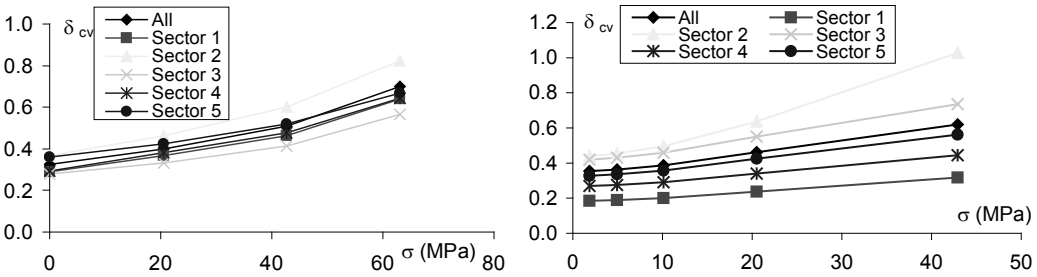

Figure 7. F1 (left) and JS1 (right) coefficient of variation of the openings versus σ.

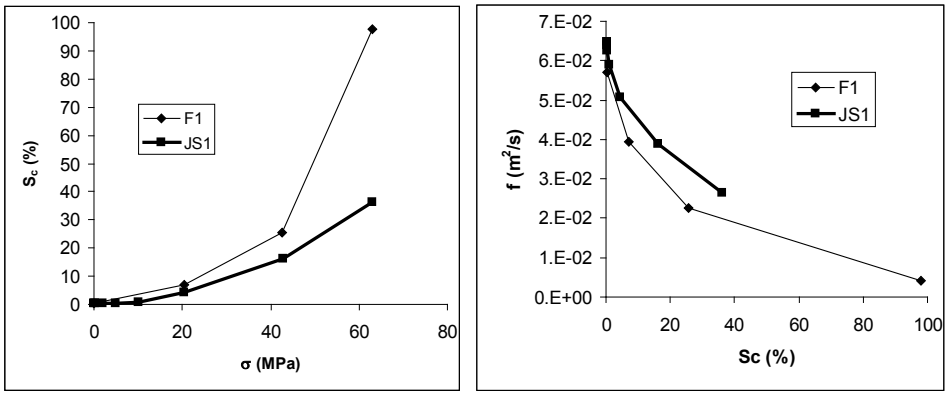

Figure 8: S_c against σ and f against S_c for F1 and JS1.

3.3 Hydro mechanical modelling

To take into account the hydro mechanical coupling effect on fracture outflow (which is not possible using the previous analytical approach), the laboratory test has been simulated using the 3DEC code. Both the fractured rock mass sample and the mortar are represented. The fracture morphology is not modelled explicitly (an equivalent fracture plane with constant initial opening is considered). This fracture however is discretised, to allow computation of different displacement, stress, pressure and flow variations from one grid point to another.

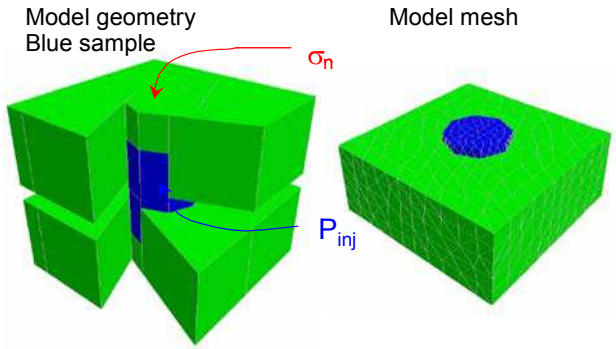

Figure 9: 3DEC model used for test interpretations

The following assumptions are done:

- the rock matrix and the fracture behave elastically. A Young modulus E = 60000 MPa, and a Poisson's ratio ν = 0.3 are assumed in coherence with the laboratory results. The analysis of the unloading phase of the tests shows that the fracture normal stiffness varies with the effective normal stress (kn = 15 GPa/m for σn = 0 MPa; kn = 80 GPa/m for σn = 20 MPa; kn = 160 GPa/m for σn = 40 MPa; kn = 240 GPa/m for σn = 60 MPa for F1 test),

- the flow inside the fracture follows the cubic law (applied on a mesh scale of the fracture). The initial value of the fracture hydraulic aperture has been determined previously from the analytical approach for zero (or small) effective stress ($a_0 = 6.10^{-5}$ m for F1 test).
- the hydraulic aperture is supposed to vary during the test according to mechanical closing Δu_n ($\Delta a = f.\Delta u_n$, where $\Delta u_n = - k_n \Delta \sigma_n'$ and f is a factor depending on the effective normal stress σ_n'). The hydro mechanical coupling is also defined by the Terzaghi/Biot relation: $\Delta \sigma_n' = \Delta \sigma_n - \beta \Delta P$. Because the hydraulic pressure variation remains small comparing to stress variation during the test, this relation has been simplified assuming $\beta=1$.

The hydro mechanical loading applied during the tests has been simplified to a series of normal stress and hydraulic pressure steps. Simulation must be regarded as a succession of steady-state calculations (one for each hydraulic pressure step). To reach balance, 3DEC carries out a certain number of hydraulic cycles, a certain number of mechanical cycles being also realized in order to obtain a mechanical balance within each hydraulic cycle. These cycles are due to the explicit character of Distinct Element Method used. Variation between measured and calculated normal displacements, observed when the normal stress exceed 40 MPa, can be explained by the fact that 3DEC does not simulate the irreversible normal displacements induced by the fracture wall damage. The computed value for the fracture outflow is highly dependent on the choice done for the ratio f between hydraulic aperture and mechanical closing variations. For each test, two simulations have been done: a first one assuming that f remain constant and is equal to 1, a second one considering the relation deter mined previously between f and σn (Figure 8).

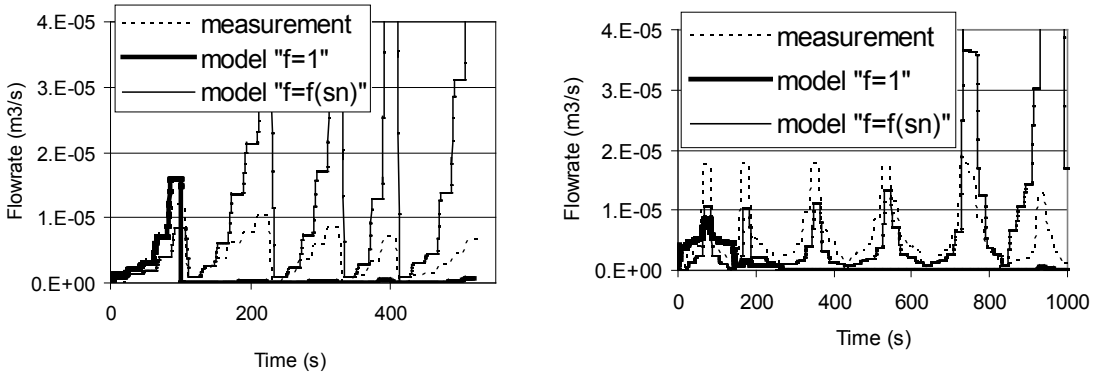

Figure 9. Comparison between measured and computed injection flow F1 (left) and JS1 (right).

When the experimental f value is injected in the model, at low normal stress levels (up to 20 MPa), there is the best fitting of the computed flow rate values with the measured flow rate values. However, the flow rate values are overestimated, especially for sample F1, for high values of normal stress and hydraulic pressure. The gap between simulated and measured flow rate can be related to the fact that the model does not take in account the fracture asperity degradation (occurring for high normal stress) and the turbulence of the flow (occurring for high injection hydraulic pressure)

4 Conclusions

After *in situ* evidence on the morphological interaction with hydro mechanical behaviour, hydro mechanical tests with morphological monitoring are performed. The back computed void spaces allow comparing, at different normal stress, the evolution of the hydraulic opening and the normal closure. The bedding planes have a lower normal stiffness than the diaclases. The values of roughness classical parameters, the range and the coefficient of variation, show that the behaviour of diaclases is stiffer than the bedding planes. When expressing the hydraulic opening raise (f) as a function of the contact surfaces, the bedding planes and diaclases have the

same variation, but this coefficient takes higher values for JS1. Furthermore, and for normal stress lower than 20 MPa, we showed that injecting the f coefficient values in the model leads to a better fit of flow rate curves. We have shown that a morphology measurement and the knowledge of the contact surface are necessary to model correctly the flow rate. However some limitations of the numerical approach used (the turbulent flow and asperity degradation are not taken into account) do not allow to reproduce closely the flow measurements. The morphology data measured during testing have not been used yet; we will use them to determinate at what normal stress value the damaging of the asperity starts, and so determinate the limit, in terms of normal stress, until the morphology measurement at the beginning of the test can be used. We need also to analyse accurately the flow between two rough joint walls, test if there is low pressure turbulence.

References

Barton N.R., Bandis S., Bakhtar K., 1985, Strength, deformation and conductivity coupling of rock joints, in International Journal of Rock Mechanics and Mining Sciences & Geomechanics Abstracts 22, 121-140.

Evans K.F., Kohl T. Hopkirk R.J., Rybach L., 1992, Modeling of energy production from hot dry rock systems, Proj Rep Eidgenössische Technische Hochschule (ETH), Zürich, Switzerland.

Goodman, R.E., 1974, The mechanical properties of joints. in Proc 3rd Int Congr International Society of Rock Mechanics, 1-7 September 1974, Denver, Colorado. National Academy of Sciences, Washington, DC, vol I, 127-140.

Hans J. and Boulon M, 2003, A new device for investigating the hydro-mechanical properties of rock joints, Int. J. Numer. Anal. Meth. Geomech., 2003; 27:513–548.

Huang T.H., Chang C.S., Chao C.Y., 2002, Experimental and mathematical modeling for fracture of rock joint with regular asperities, in Engineering Fracture Mechanics, vol. 9, 1977-1996.

Lee S.D., Harrison J.P., 2001, Empirical parameters for non-linear fracture stiffness from numerical experiments of fracture closure, in International Journal of Rock Mechanics and Mining Sciences 38, 721-727.

Londe P., Sabarly F., 1966, La distribution des perméabilités dans la fondation des barrages voûtés en fonction du champ de contrainte, in Proc 1st Congr Rock Mechanics, 25 septembre-1 Octobre 1966, Lisbon. Lab Nac Eng Civil, Lisbon, vol II, 517-522.

Nazridoust K., Ahmadi G., Smith D.H., 2006, A new friction factor correlation for laminar, single-phase flows through rock fractures, in Journal of Hydrology, Volume 329, p. 315-328.

Qian J., Zhan H., Zhao W., Sun F., 2005, Experimental study of turbulent unconfined groundwater flow in a single fracture, in Journal of Hydrology, Volume 311, Issues 1-4, 15 September 2005, 134-142

Rutqvist J, Stephansson O., 2003, The role of hydromechanical coupling in fractured rock engineering, in Hydrogeology Journal 11, Springer-Verlag (Ed.), 7-40.

Witherspoon P.A., Wang J.S.Y, Iwai K., Gale J.E., 1980, Validity of cubic law for fluid flow in a deformable rock fracture, Water Resour Res 16 , 1016-1024.